Hindawi
Shock and Vibration
Volume 2019, Article ID 2621092, 13 pages
https://doi.org/10.1155/2019/2621092

Research Article

Effective Processing of Radar Data for Bridge Damage Detection

Tomasz Owerko and Przemysław Kuras

Department of Surveying Engineering and Civil Engineering, AGH University of Science and Technology, Kraków 30-059, Poland

Correspondence should be addressed to Tomasz Owerko; owerko@agh.edu.pl

Received 4 January 2019; Revised 12 March 2019; Accepted 20 March 2019; Published 17 April 2019

Guest Editor: Elías López-Alba

This paper presents the practical results of the evaluation of the data obtained by using ground-based radar interferometer during measurements carried out on bridge structures. Due to the nature of the objects studied, the authors proposed a comprehensive method of data analysis, which identifies whether the passage of the vehicle did not damage the bridge. The effective use of vehicles as a source of bridge excitation allowed us to first develop a method for determining the damping parameters resistant to potentially occurring beating frequencies. As a result, it is possible to determine these subsets of data registered with radar, for which it is possible to assume compliance with linear systems. This type of data, often omitted in other works, forms the basis for the second important element of the research—an algorithm based on the ARMA model supporting defect detection. The optimization of the performed calculations, in particular the proposed optimal ARMA model order, the method of fault identification based on the DSF parameter, or fault identification based on a nonmetrical Cook's distance leads to a robust and scalable method. The method's low computational complexity allows for implementation in real-time solutions. In addition, the distribution of errors and the sensitivity of classifiers based on the DSF parameter and Cook's distances leaving them will enable the automation of the classification process using machine learning. The proposed method is universal; in particular, it can be used for radar interferometry methods because it is resistant to potentially variable environmental conditions.

1. Introduction

The inspection measurements of important and non-standard engineering structures and related studies are the basis for assessing their safety. In the group of objects that must be monitored during load tests and require monitoring are, among others, bridge structures and buildings exposed to the influence of seismic factors. The monitoring of such facilities and their examination under test loads should provide a basis for assessing the safety of the structure at the time of its commissioning and in the future.

Many failures can be identified based on the analysis of observations carried out using various measuring devices. In this group, attention should be paid to the radar interferometry technique that allows simultaneous observation of many elements representing the tested structure. Its important advantage is the ability to conduct measurements in a noncontact manner and that there is no requirement to install any devices on the object.

The use of radar observations of many points on the site to analyze the health of the structure is quite wide. This type of research is carried out for both bridge and high-rise buildings by determining the vibration parameters based on dynamic displacement monitoring [1]. Gentile and Bernardini [2] describe the application of the radar sensor to vibration full-scale measurements of a bridge in relation to the time series recorded by the conventional accelerometers. In this research, the application of the radar sensor to vibration full-scale measurements of a bridge in relation to the time series recorded by the conventional accelerometers is presented. As a result, the resonant frequencies and mode shapes of the bridge that were identified from the radar signals are compared to the corresponding quantities estimated from the data recorded by the conventional sensors. Moreover, Barros and Paiva [3] present many different types of bridge structures on which radar measurements were performed as a part of SHM. For each case study, the comparison with the akin results obtained for the same case studies either by structural computational modeling or by other intrusive SHM techniques is described, in order to ascertain the accuracy of this nonintrusive radar interferometry. In turn, Diaferio et al. [4] focus on operational modal analysis (OMA), which is extensively used as a tool for the modal identification and the SHM of civil engineering constructions. They analyze the capability and the possibly needed improvements of the ground-based radar interferometric experimental set-up applied to a railway viaduct, as an alternative to classical experimental techniques based on the use of accelerometers, which involve high costs and long times for performing measurements and often interrupt the service of a construction. Another example of the application of radar measurements in relation to the alternative observational method, which is a vision-based measurement system based on the digital image correlation coefficient, is presented by Kohut et al. [5]. This research was carried out to assess the behavior of the tram viaduct as a result of operational loads.

Research on the condition of structures based on radar observations has also been carried out for high objects. Hu et al. [6] use radar measurements to high-rise building observations. They established a sequential quadratic programming-genetic algorithm to identify the dynamic vibration characteristics of buildings under natural environment excitation. This method not only accurately identifies resonance frequencies but also directly extracts the amplitudes of the sine and cosine components of the building vibration signals under the resonance frequencies response compared with the traditional spectrum analysis based on the fast Fourier transform.

Another example is a historic masonry bell tower examined by Castellano et al. [7]. The proposed approach exploits the extraction of modal parameters to define mechanical features of the structure such as mass, damping and stiffness matrices by means of operational modal analysis, starting from measurements performed by a very promising, expeditious, and contactless experimental technique based on radar interferometry. This approach may be very effective for structural health monitoring purposes. A different application is presented by Ochieng et al. [8]. They used a noncontact radar observation for structural health monitoring of infield wind turbines blades. Radar sensor helps the monitoring of blades during design, testing, and operation. Furthermore, it supports the determination of damage detection for infield wind turbine blades within a 3-tier SHM framework especially for those made of composite materials by way of condition parameter residuals of extracted modal frequencies and deflection.

Damage detection is one of the most important applications of SHM systems and algorithms. Modern computational technologies based on digital signal processing, the evaluation of patterns by means of machine learning, or the evaluation of patterns by the analysis of statistical characteristics of signals can be used to assess the safety of building objects [9, 10].

Recently, an important trend in this field is the use of machine learning to identify potential problems. While the use of AI methods is widely known for systems based on the analysis of dynamic data, it is also worth noting that it is possible to effectively analyze data from high-resolution measurement systems using deep machine learning methods [11]. The use of photogrammetric systems and computer vision systems can also successfully include dynamic measurements. This type of work encompasses many research directions, among which the following should be mentioned: different template matching techniques for tracking targets, coordinate conversion methods for determining calibration factors to convert image pixel displacements to physical displacements, measurements by tracking artificial targets vs. natural targets, and many others.

Finally, the applications of the measured displacement data for SHM are reviewed, including examples of structural modal property identification, structural model updating, damage detection, and cable force estimation [12]. An important element of SHM systems is not only to identify the damage but also to give such information an adequate weight. In particular, research work may include the provision of information on the SHM system including the number of sensors and sensor locations [13]. The complexity of SHM systems and a large number of sensors do not remain indifferent to the possibilities of the efficient use of systems.

As important as research work that focuses on system reliability, there are those that aim to reduce computational complexity while maintaining damage detection efficiency. In particular, unlike conventional strategies employing a frequency response function or response data, a damage detection methodology is addressed by employing transmissibility functions that retain a strong interrelation with structural damage or deterioration in order to avoid the measurement of excitation, together with the principal component analysis that leads to a reduction in computational costs [14].

Studies on SHM algorithms concern, just like in this paper, the identification of damages occurring on bridge structures. These tests, which are crucial for practical applications, must also include an analysis of the interaction between the bridge and the vehicles that constitute the source of disturbances and vibrations [15]. Long-term monitoring of objects is inherently subject to changing environmental conditions, in particular to changing weather conditions. Such changes affect both the measurement system and the behavior of the object itself. Huang et al. [16] address this problem by indicating that, in practical applications, time-varying environmental and operational conditions, such as temperature and external loadings, often overwhelm the subtle changes caused by damage. It is therefore of great significance to remove those structural changes (damage features) caused by external influences from actual structural damage. The authors present a new damage identification method based on the Kalman filter and cointegration (KFC). As a result, the environmental effects on a damage indicator are removed, thanks to the cointegration process of the Kalman filtered coefficients. Bhowmik et al. [17] show that most work to date deal with algorithms that require windowing of the gathered data that render them ineffective for online implementation. Algorithms focused on mathematically consistent recursive techniques in a rigorous theoretical framework of structural damage detection are missing. This motivates the development of the present framework. As a solution, a baseline-free approach for continuous online damage detection of multidegree of freedom vibrating structures using recursive singular spectral analysis in conjunction with time-varying autoregressive modeling is presented. Besides, the problem of long-term monitoring is also considered by Roy et al. [18]. The authors draw attention to the fact that a direct comparison of the vibration signals or modal properties at different periods of time may not be sufficient to identify the damages and their locations. Therefore, it is important to analyze the vibration signals to extract the morphologies of the changes in these response signals and correlate them with the types, location, and magnitude of structural damage.

An interesting solution, presented by Krishnan et al. [19], successfully eliminates the need for offline post-processing and facilitates online damage detection especially when applied to streaming data without requiring any baseline data. This is a novel baseline-free approach for the continuous online damage detection of multidegree of freedom vibrating structures using recursive principal component analysis (RPCA) in conjunction with time-varying autoregressive (TVAR) modeling. In this method, the acceleration data are used to obtain recursive proper orthogonal components online using the rank-one perturbation method, followed by TVAR modeling of the first transformed response, to detect the change in the dynamic behavior of the vibrating system from its pristine state to contiguous linear/nonlinear states that indicate damage.

On the contrary, the health analysis of the structure based on data representing the stationary parts of measurement signals has been presented, among others, by Sohn et al. and Nair et al. [20, 21]. They are an important element in the proposed solution.

This work presents an algorithm for conducting research under testing or operational load that allows simultaneous observation which will allow for identifying any structural damage that may occur during testing and are the basis for building a reference database of the system based on SHM.

An algorithm for detecting and automatically identifying the defects of buildings and structures is applied. It is particularly useful for engineering structures susceptible to dynamic excitations such as bridges, viaducts, flyovers, masts, and towers, as well as free-standing chimneys (single and multi-flue) based on tests carried out under testing or operational load.

2. Proposition of the Damage Detection Algorithm

2.1. Overview. The computational technique is that the measurement signals, which are variable in time, are measured, and the results are delivered to the computing unit in the form of time series and spectrograms, and analyses are carried out for the stationary fragments of the time series.

In the first stage, when measuring a given structure, measuring devices, such as the accelerometers, interferometric radar, or GNSS receivers, are positioned in such a way that the following can be performed:

(a) It is possible to accurately identify the mode shapes resulting from the modal analysis of the structure

(b) They are located in the places that are subject to damage during tests under test loads and operational loads

In the second stage, the values of the identified amplitudes obtained from those parts of the time series, which represent free vibrations, are compared with the results of the modal analysis in the range of values in the frequency domain and in the range of the logarithmic decrement of damping calculated from the Hilbert transform of free vibration [22].

Then, in the parts of the time series that represent the stationary signal, the ARMA model is fitted (a linear model of autoregressive moving average) [23]. On this basis, the damage sensitive feature (DSF), introduced by Nair et al. [21], is calculated as the normalized value (the first coefficient is divided by the square root of the sum of the squares of the first three coefficients).

In the third stage, it is calculated if the distance of the given calculated coefficient, on the basis of the given time series after the crossing of a vehicle, changes the coefficients of the regressive lines fitted into the previous realizations of the DSF with the use of Cook's distance. In this way, the dynamic behavior of the bridge, which deviates from the norm, is identified.

The signal recorded during the load testing can be divided into three parts in the time domain (Figure 1):

(1) The data represent the stationary signal. This is the basis for finding the structure's features representing its condition prior to possible damage and in the parts representing the condition of the object after free vibration has expired. The second part is the basis for evaluating whether or not the force damaged the object.

(2) The data represent the deflection of the construction. The standard procedure may be used to calculate other parameters such as the coefficients of the dynamic amplification factor (DAF).

(3) The data represent the free vibration. The correctly filtered and standardization process allows for the calculation of an amplitude spectrum and also may determine if the design is acting in accordance with the damping based on the values of the logarithmic decrement of damping.

2.2. Estimation of the Structure Damping. It is common practice to use free-damping data to verify FEA (finite

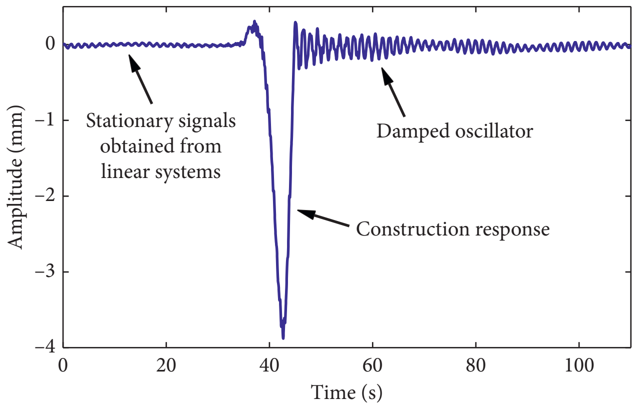

Figure 1: The decomposition of the measurement signal (reproduced from [24], under the Creative Commons Attribution-NonCommercial 4.0 International License).

element analysis) models. Usually, data are used to obtain information about the amplitude spectra (Figure 2). In order to correctly establish an amplitude spectrum, the incoming signal must be processed with a band-pass filter supported by data and a precalculated modal analysis based on the finite elements analysis method. The interval representing free vibration may be presented as follows:

$$x(t) = Ae^{-Bt}\cos(\omega t + \varphi), \quad (1)$$

where A is the amplitude, B is the damping coefficient, ω is the frequency, φ is the phase, and t is the time.

If a Hilbert transform was calculated for such a signal, the envelope of the damped oscillator was obtained as a result (Figure 3).

Taking into account equation (1), the estimated parameter B may be calculated in the following two ways:

(i) Directly from the definition by fitting the exponential function into the result of the Hilbert transform

(ii) By fitting the linear function into the logarithm of the Hilbert transform

A classic logarithmic decrement of damping is calculated upon the basis of the following equation:

$$\delta = \ln\frac{A_n}{A_{n+1}}, \quad (2)$$

where δ is the logarithmic decrement of damping and A_n and A_{n+1} are the consecutive amplitudes.

The direct use of equation (2) does not solve the problem, which is illustrated in Figure 3. Although the band-pass filter is used, the signal, which registers the free vibration, is affected by two very similar frequencies because the phenomenon of beat frequencies occurs in bridge structures while being tested. Such a situation is found on bridge structures, especially for cable bridges [10, 25, 26]. The proposed solution of this occurrence is superior to the classical method based upon the definition of the logarithmic decrement of damping that, in the submitted example, the estimation of the damping coefficient is not

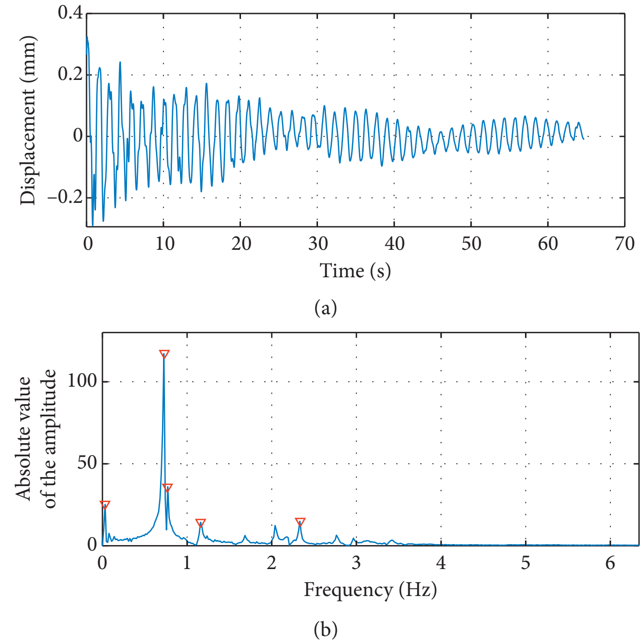

Figure 2: Example of time series and its amplitude spectrum (reproduced from [24], under the Creative Commons Attribution-NonCommercial 4.0 International License).

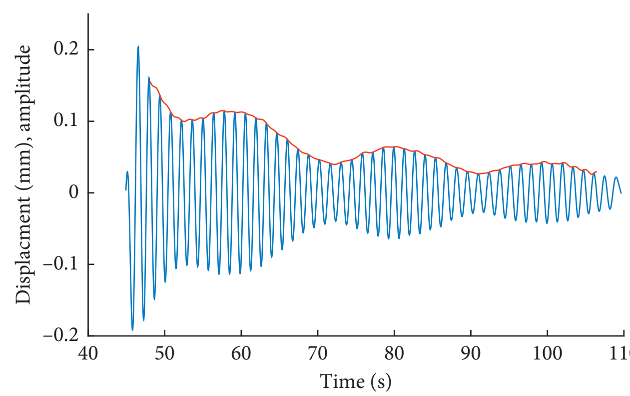

Figure 3: Hilbert transform calculated for signal obtained from damping vibrations with beat frequencies (reproduced from [24], under the Creative Commons Attribution-NonCommercial 4.0 International License).

hampered by the errors occurring from the number of frequency components (Figure 4).

The standard equation describing the vibration is exponential. It is by its nature difficult to be analyzed by regression algorithms. The proposed solution is based on linearizing the equation before estimating the parameters. The logarithmic representation of the Hilbert transform can be easily estimated using linear regression or generalized linear regression with selected cost function (the authors present the use of LSF as a cost function). It is a more effective way and a more robust solution.

Such an approach allows for the estimation of the damping coefficients to be based on a robust estimation. In addition, while the estimation is being determined, the entire

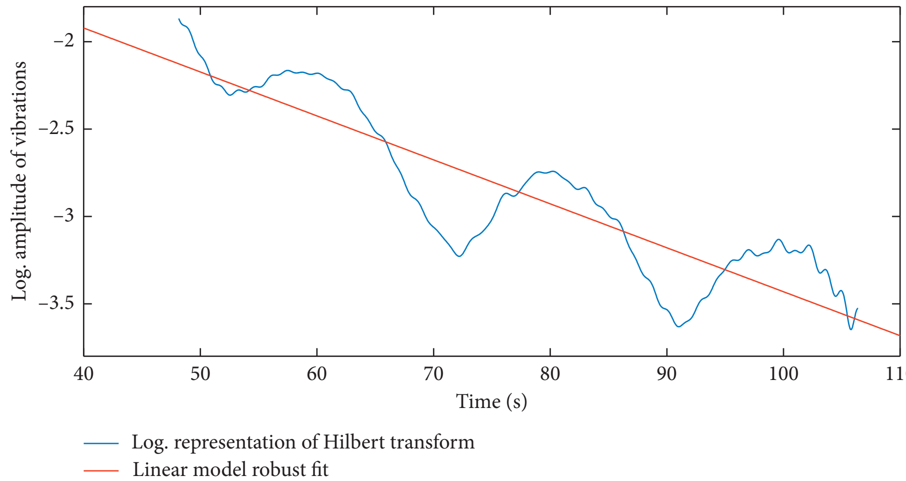

FIGURE 4: Logarithmic representation of Hilbert transform (blue) and linear estimation (red) (reproduced from [24], under the Creative Commons Attribution-NonCommercial 4.0 International License).

data acquisition of the measuring signal is being utilized, rather than an arbitrarily chosen amplitude (Figure 4). Therefore, after determining the linear estimation,

$$y = Bx + C, \tag{3}$$

$$\delta = B \cdot T, \tag{4}$$

where T is the period of the dampened vibration and C is the constant.

2.3. Structural Health Estimation and Damage Detection. If during a load test, damage to the construction occurred, it would change the statistical characteristics of the measured data. There exists a group of methods which has been developed for the identification of the damage. They are based on the congruency of the ARMA (autoregressive moving average) models into the given data. The general form is as follows:

$$x_{ij}(t) = \sum_{k=1}^{p} a_k x_{ij}(t-k) + \sum_{k=1}^{q} b_k \varepsilon_{ij}(t-k) + \varepsilon_{ij}(t), \tag{5}$$

where $x_{ij}(t)$ is the normalized measurement signal, a_k and b_k are the k-th AR and MA coefficients, p and q are the model orders of the AR and MA processes, and $\varepsilon_{ij}(t)$ is the residual term.

The algorithms of the group are discussed in detail [10, 19, 20]. In particular, the modified and implemented algorithm adapts to the structure in Figure 5.

The structure of the proposed algorithm is discussed in more detail below. The assumption is to answer the question whether the condition of the structure before the vehicle's approach during the loading of the bridge structure and after that has changed. The algorithm operates on data portions—called batch or data intervals. Batch data processing is an efficient way of processing high volumes of data where a group of transactions is collected over a period of time. Data are collected, entered, and processed, and then the results are produced. Since we would like to be able to compare the

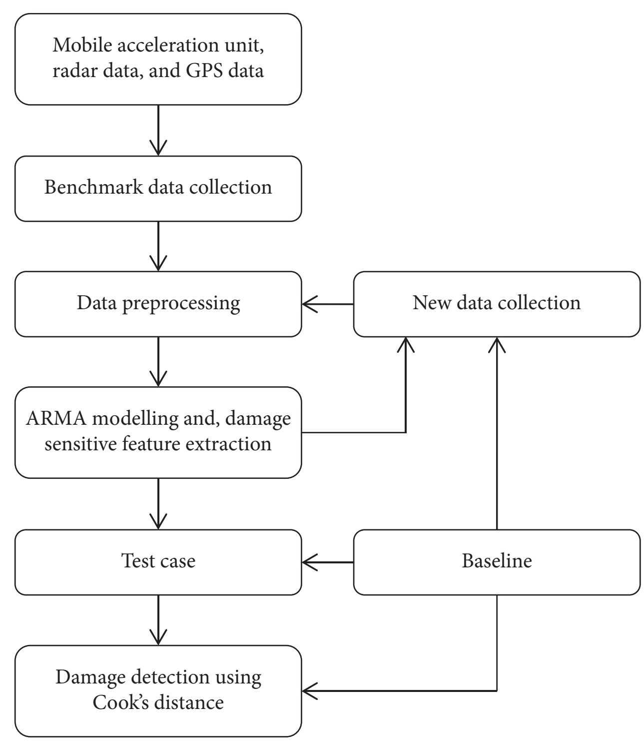

FIGURE 5: Selected and implemented ARMA algorithm framework.

results between measurements, the intervals of the data must be standardized in the beginning of the process, as is shown in Figure 5. A practical way of doing this is as follows:

$$\overline{x}(t) = \frac{(x(t) - m)}{\sigma}, \tag{6}$$

where $x(t)$ is the analyzed interval (batch of data), m is the mean value, and σ is the standard deviation.

After the standardization, the time series is entered into the model of ARMA in accordance with equation (5). Taking into consideration the different types of engineering structures, the rank of the coefficients AR (p) and MA (q), in the proposed solution, is subject to estimation.

Therefore, the effect of the action of the algorithm will be the result of the damage sensitive feature of the DSF parameters calculated for the specific data vectors representing the engineering structure before and after the potential damage (Figure 6):

$$\mathrm{DSF} = \frac{a_1}{\sqrt{a_1^2 + a_2^2 + a_3^2}}, \quad (7)$$

where a_i is the coefficients obtained from equation (5).

The classical approach to identify the damage in a given structure is that one must take all the obtained DSF coefficients prior to the test (marked in Figure 6 as circles) and use this as a basis to calculate the estimated value. The next step would be an analogical procedure for the entire interval representing the structure behavior after the excitation has been applied to the construction (the result is marked in Figure 6 as plus signs).

Hence, for both groups of data, the mean values have to be estimated. Upon this basis, it may be concluded that there will be a substantial difference between the groups, using the standard t-test for this aim.

This type of approach has two characteristic shortcomings:

(1) It is crucial to take a sufficient number of samples representative of the structures behavior after force has been applied to the construction, in order for the statistical significance from the given test to be properly kept at accordingly a high level.

(2) Limiting the possibility of using the calculation techniques of bridge structures while under operation being subjected to continual use, there may not be a suitable length of time between the impact of the structure to gather the proper amount of data to run a t-test determining the DFS coefficients.

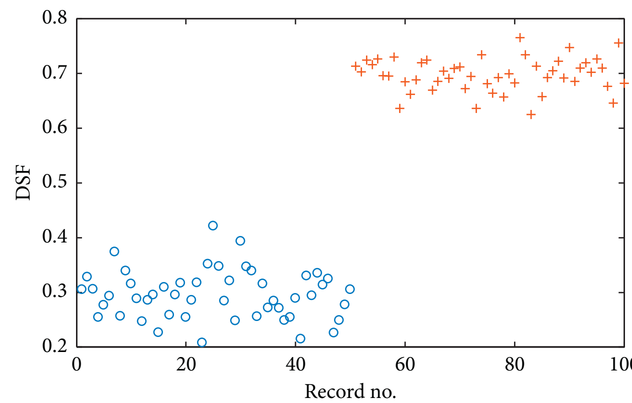

Figure 6: DSF obtained from example data (reproduced from [24], under the Creative Commons Attribution-NonCommercial 4.0 International License).

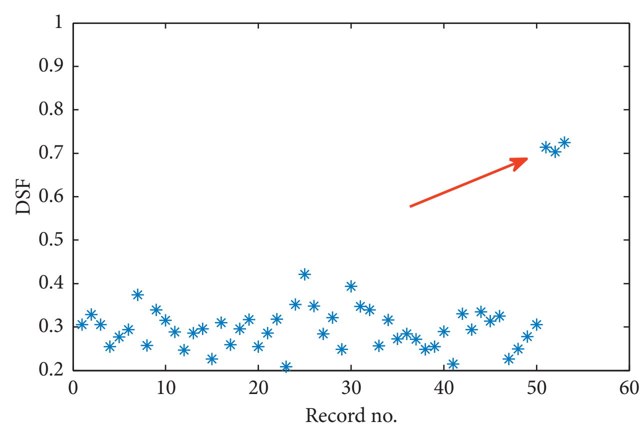

Figure 7: DSF obtained from object with limited data after extraction (reproduced from [24], under the Creative Commons Attribution-NonCommercial 4.0 International License).

2.4. Reducing the Amount of the Necessary Data. The abovementioned limitations may be solved by using a different criterion than the statistical difference estimated between the two groups of data. A dataset was considered in which after the excitation and damping of the object and before the next excitation, a limited amount of data can be registered. It means that two consecutive forces are applied to the structure in a short time. In the case of such data, it is possible to calculate a limited number of the DSF coefficients (in Figure 7 marked with an arrow).

Such a situation may be encountered when research is being carried out in bridge structures that are in current use, especially those with a large variety of vehicles that are not standard and are oversized. The question at hand is whether or not a given vehicle may be the cause of damage to a structure even during minimal intervals between the impacts.

In order to verify whether the limited number of DSF parameters that were registered are significantly different from the average realization, the formula that may be used in such a regression analysis is based upon Cook's distance given by the following equation:

$$D_i = \frac{\sum_{j=1}^{n} \left(y_j - y_{j(i)}\right)^2}{p \cdot \mathrm{MSE}}, \quad (8)$$

where y_j is the j-th fitted response value, $y_{j(i)}$ is the j-th fitted response value where the fit does not include observation i, MSE is the mean squared error, and p is the number of coefficients in the regression model.

There are several reasons why Cook's distance has been chosen as a tool to detect changes in the DSF coefficients value. First of all, the use of this method allows for the diagnosis of the object's state immediately after the load has been removed which is crucial for the algorithm. Thus, the potential damage to a bridge object can be detected on the basis of a small amount of data. Second, there are unambiguous, objective criteria for assessing whether Cook's persistence is statistically significant [27]. Thirdly, it is not necessary to perform recursive statistical significance tests of the DSF coefficients, which significantly reduces computational complexity.

Figure 8 presents Cook's distances calculated for the example dataset. It is easy to see that all of the captured DSF

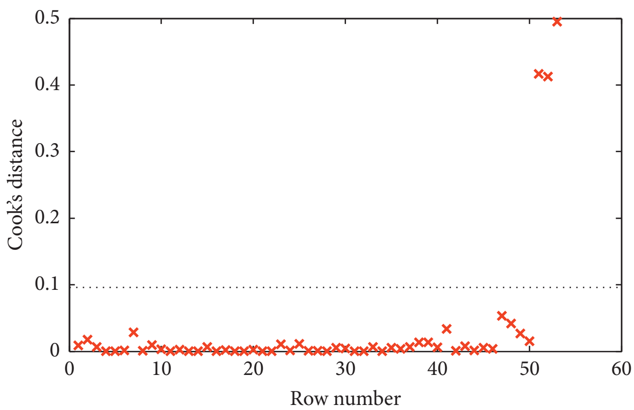

Figure 8: Cook's distance calculated for the linear model of DSF coefficients [24] (reproduced from [24], under the Creative Commons Attribution-NonCommercial 4.0 International License).

coefficients for the vectors of the data representing a damaged structure are assigned a value above line.

The dashed line in Figure 8 corresponds to the recommended threshold value of three times the mean of Cook's distance. The plot has observations with Cook's distance values which are greater than the threshold value. In particular, the DSF obtained for vector numbers 51, 52, and 53 have Cook's distance values that are relatively higher than the others, which exceed the threshold value. Usually you might want to find and omit these from your data and rebuild your model, but in our case, this information is used to answer the question if extraction (for example, a vehicle) caused damage to the tested bridge. It is important to keep in mind that this is not the value of Cook's distance, but the change in the value of the DSF coefficient is the basis for identifying the damage to the object. Cook's distance is only a tool that allows you to objectively and efficiently find changes in the DSF value.

3. Bridge Test Results

3.1. Acquisition of the Observation Data. The object on which the test was carried out was a tram viaduct. The ground-based interferometric radar IBIS-S was used to acquire the data (Figure 9). The displacements of a dozen points representing the bridge span were the subject of measurement; however, the observations of one point, located in the span half-length, were used for further analyzes. The sampling frequency was set as 100 Hz.

The design specifications on the phase accuracy applied on the radar system, which was used in the presented research, are suitable for measuring short-term displacements with a range accuracy better than 0.1 mm [28]. Moreover, the radar manufacturer claims that displacement surveying accuracy is at the level of 0.01 mm. This value is confirmed by the analyses carried out by Rödelsperger [29], who consider the relationship between the SNR (signal to noise ratio) and the displacement measurement error. The SNR value depends on the intensity of the radar signal reflected by the observed object. For an SNR of 40 dB, the displacement measurement error is 0.03 mm and decreases with a further

Figure 9: IBIS-S radar unit under the tested bridge span.

increase of SNR. The time series subjected to further analysis was recorded for one of the 7 points observed on the bridge span, and for all of them, the SNR was greater than 65 dB.

In the conducted research, it was assumed that the impact of the atmospheric disturbance and the multipath signal effect is negligible. This is possible because, during the observation, the atmospheric conditions did not change and the configuration of the measurement system and the object remained unchanged. In addition, taking into account the fact that the precision of the measurement result is more important to the performed tests than its accuracy, it may be assumed that the record of 0.01 mm displacement is an actual observation.

The time series subjected to further analysis is shown in Figure 10. The data representing the stationary signal are marked in red. They provide input data for the proposed algorithm for potential damage detection. With the use of arrows, the intervals of clear excitation of the free vibrations are marked, which will be used to determine the frequency spectrum of the construction vibrations and the logarithmic decrement of damping.

In the proposed algorithm, the frequency spectrum analysis is not a key but an auxiliary element of the solution. The essence of the algorithm is based on the transformations of stationary signals. However, the proposed application of the method is monitoring bridges that will be subjected to vehicle traffic. Therefore, in order to correctly analyze the data, it is necessary to verify when after the excitation the construction vibration has been damped.

To determine the parameters of damping the structure, the observation intervals marked with arrows were used (Figure 10). The selected observation intervals were subjected to FFT analysis. Both of the analyzed cases showed a dominant frequency of value 2.95 Hz ± 0.01 Hz. This means that the natural vibration period of the tested bridge span is $T = 0.34$ s.

According to the proposed algorithm, the Hilbert transform was used to determine the damping of the structure. The signal from the observation is marked in blue, while the envelope of the vibration (i.e., the graph of the Hilbert transform) is shown in red (Figure 11).

Then, in the logarithmic representation of the Hilbert transform, the linear function was fitted (Figure 12). The determined value of parameter B defined in equation (3) is

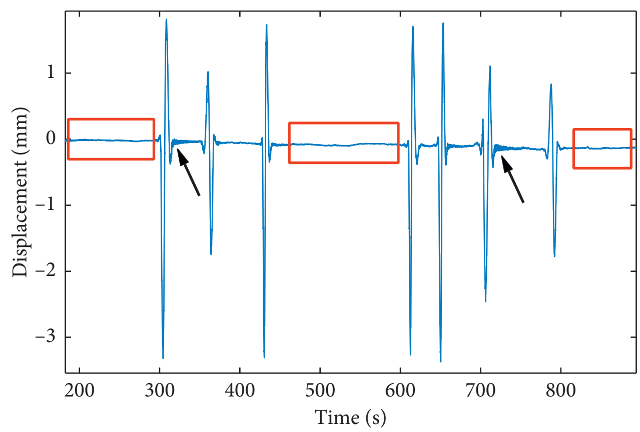

Figure 10: Data input for time-series-based damage detection algorithm (searching for stationary signals using selected parameters of object damping).

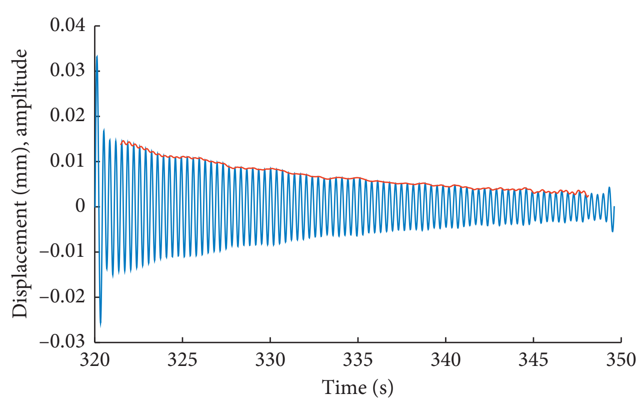

(a)

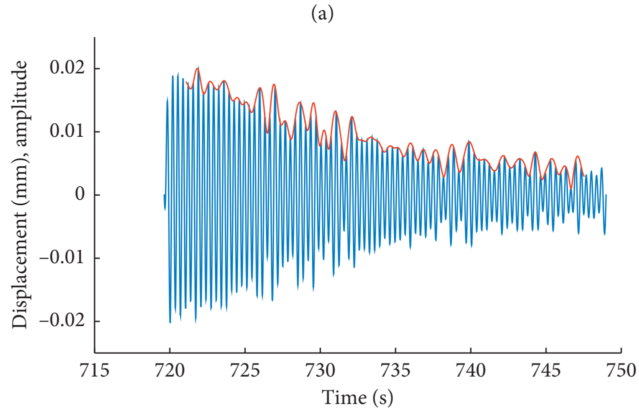

(b)

Figure 11: Hilbert transform of selected intervals.

0.0572 and 0.0646 for the analyzed cases. This means that the logarithmic decrement of damping equals 0.019 and 0.022, respectively.

3.2. Optimization of Algorithm Parameters. The algorithm of the structure damage detection based on the autoregressive moving average model has several parameters that can be adjusted adequately to the analyzed building objects. Among them are the p and q values, that is, the model orders of the AR and MA processes can be pointed out. In addition, the length of the vector containing the data to determine the DSF parameter is also not strictly defined, the same as the number of these vectors. Hence, for the analyzed case, an attempt was made to determine the optimal AR and MA values (Figures 13 and 14, respectively).

In the following figures, different symbols were used for marking the DSF values obtained as a result of the analysis of the signal recorded before the occurrence of the load and after the load termination and related effects (like the damped vibrations). The solid lines in the corresponding colors represent the regression lines fitted into the set of DSF values determined for the adopted number of the analyzed data vectors.

The values of the model orders of the AR and MA processes have a range that makes them appropriate for the analysis [21]. The presented variants allow the choice of $p = 4$ and $q = 3$ as optimal for further analysis. And while the q parameter does not significantly affect the DSF values ($q = 3$ was chosen for further analysis), in the case of parameter p, the differences are significant. The choice of $p = 4$ for further analysis is due to the smallest variability of the DSF value (the black markers in Figure 13) in relation to the time series from the observation of the structure before the load occurrence, i.e., the potential damage.

In the next stage, the effect of the length of the vector containing the data to determine the DSF parameter and the number of analyzed vectors was verified. Observation data were divided into two ways: (1) 21 vectors with 200 elements and (2) 11 vectors with 400 elements (Figure 15). The results indicate a higher sensitivity of the variant (1); however, the variant (2) also reveals that the values are significantly different from the average. This is important in the process of detecting changes in the state of the structure. The advantage of variant (2) is the higher calculation speed.

3.3. Application of Cook's Distance. In the proposed algorithm, Cook's distance was used to determine if the implementation of a limited number of DSF parameters are significantly different from the average realization. The analyses were made on the basis of the DSF datasets, as shown in Figure 15. The effect is shown in Figure 16. The DSF values exceeding the adopted threshold (the dashed lines in Figure 16), i.e., the outliers, are marked with red circles.

It should be noted that the DSF values that would indicate a change of the structure state (vectors no. 9–13 in Figure 15(a) or vector no. 6 in Figure 15(b)) are not confirmed by the calculated Cook's distance. On the contrary, there can also occur outliers (the black cross in Figure 16(b)) which do not indicate damage on the basis of the DSF. This leads to the conclusion that the detection of structural damage should be based not only on the DSF coefficient but also on Cook's distance, which is its valuable complement in the proposed algorithm. The proposed algorithm has an advantage over a standard solution because it is not based on simple statistical significance testing of the DSFs. As a result, the size of the sample before and after the load can vary.

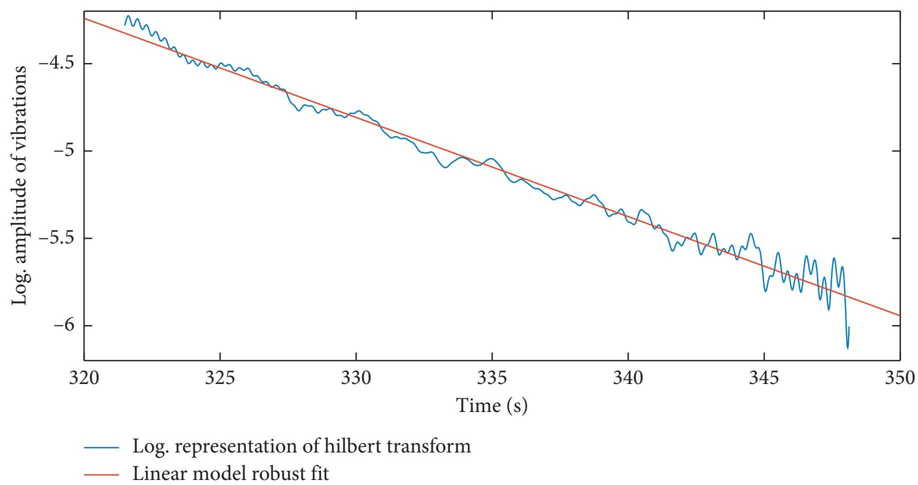

(a)

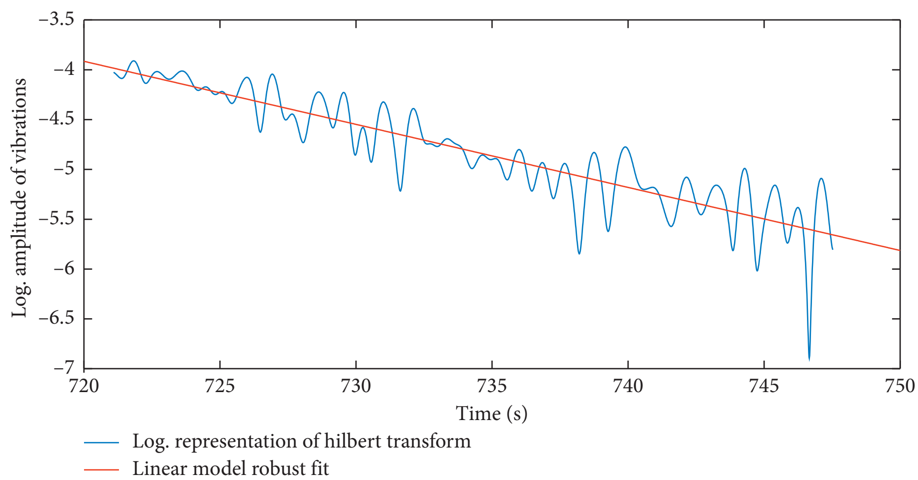

(b)

Figure 12: Logarithmic representation of Hilbert transform.

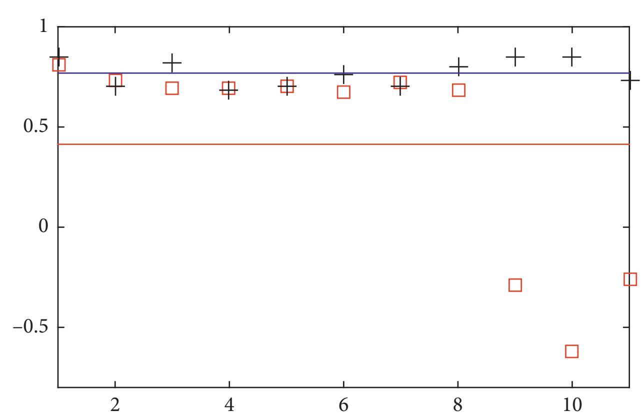

(a)

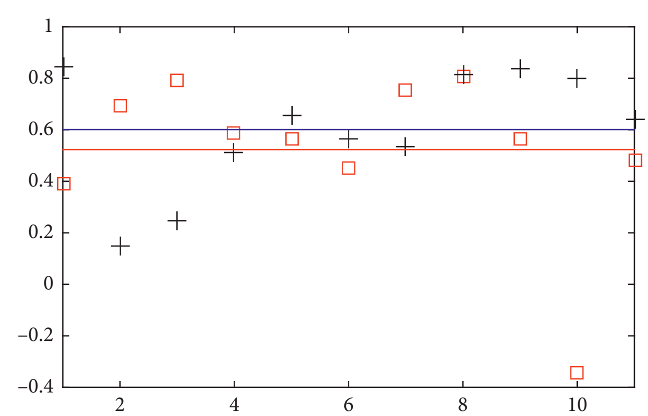

(b)

Figure 13: Continued.

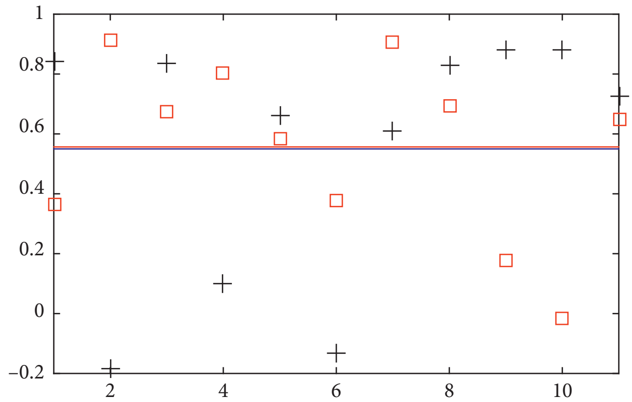

(c)

Figure 13: Distribution of DSF values depending on the AR process order: (a) version order of AR = 4, order of MA = 3; (b) version order of AR = 5, order of MA = 3; (c) version order of AR = 6, order of MA = 3.

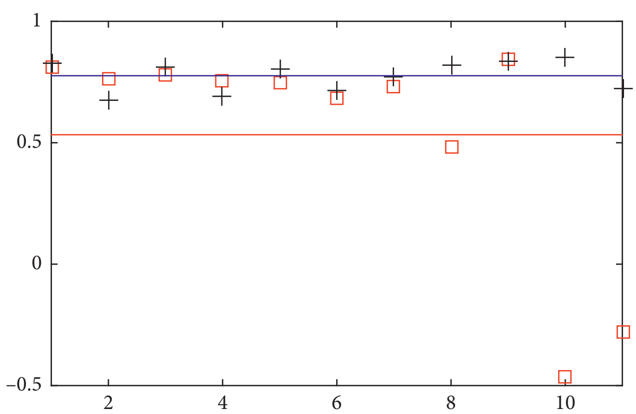

(a)

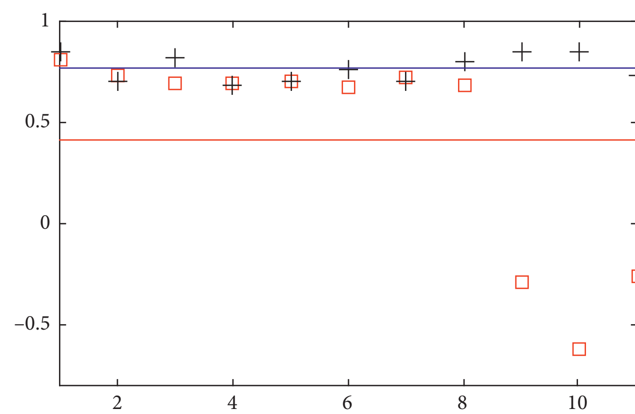

(b)

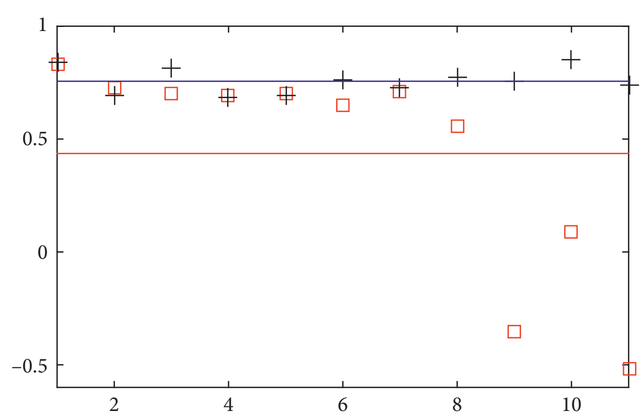

(c)

Figure 14: Distribution of DSF values depending on the MA process order: (a) version order of AR = 4, order of MA = 2; (b) version order of AR = 4, order of MA = 3; (c) version order of AR = 4, order of MA = 4.

It also does not matter what the distribution of the residuals is (there is no need to meet the assumptions related to a formal significance test). In the examples discussed, the values of the DSF coefficients signaling object damage are unlikely to be detected by another method. Thanks to this, the proposed method is not only faster but also more sensitive.

4. Conclusions

The presented algorithm comprehensively discusses the methods of prototyping engineering structures, in particular, examining bridges under testing and operational loads. Its basic assumptions and features are the following:

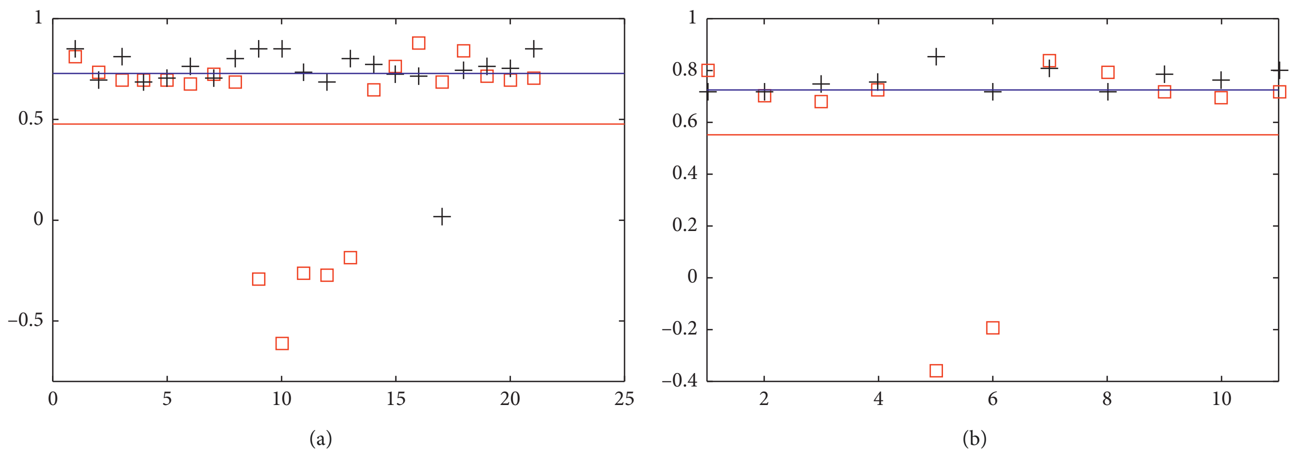

Figure 15: Analyzed cases of vector length: (a) version order of AR = 4, order of MA = 3; (b) version order of AR = 4, order of MA = 3.

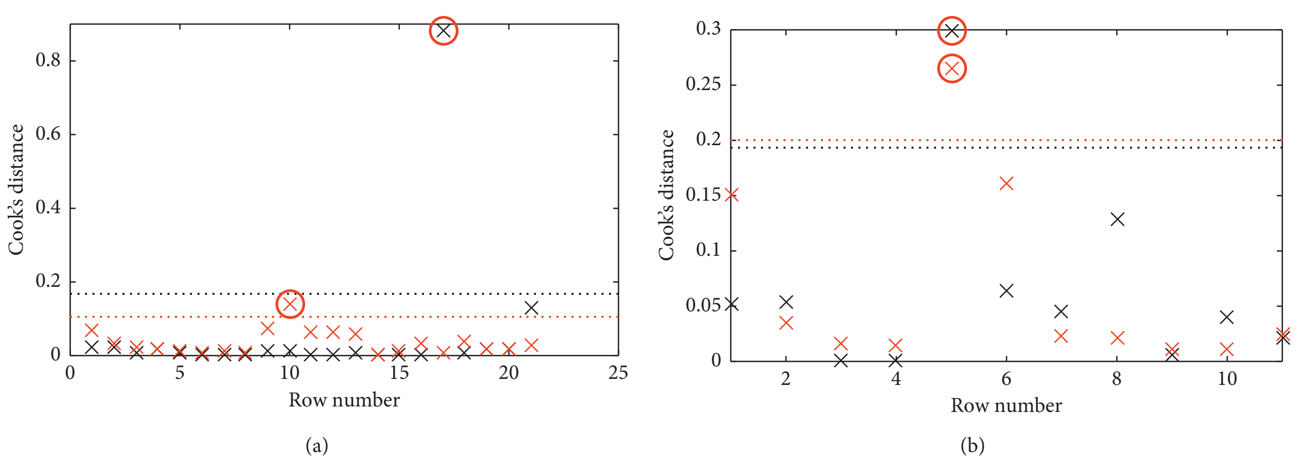

Figure 16: Distribution of the DSF values depending on the order of the MA process.

(1) The decomposition of the recorded signal represents the vibration of a given bridge structure into three groups in the time domain. The first group contains data before an impact and after free vibration, and technically, it is the group of stationary signals of linear systems. The second group is the response of the construction (i.e., the deflection of the span occurred). The third group is the part of the signal which represents the free vibration in a structure that is excited.

(2) The decomposition of a signal in a frequency spectrum, especially with band-pass filters, allows for the more effective spectral analysis. The band width is the results of the FEM analysis.

(3) The amplitude spectrum is comparable to the analysis made with the finite elements method through the calculation of the fast Fourier transform.

(4) Construction damping of an object is represented by the logarithmical decrement. The calculation of its values is not dependent upon the implementation of the direct definition but on the calculation of the Hilbert transform. Furthermore, for the logarithm of the envelope, the linear regression with the robust least squares fitting method is calculated. The calculated coefficients of the linear estimation allow for an estimation of logarithmic decrement of damping in the entire signal, even when the structure experiences beat frequencies.

(5) The identification of the potential damage to a structure as a result of impact is based on the DSF coefficients. The answer to the question if the damage occurred is based on Cook's distance rather than the comparison of the average values of the tests is obtained as follows: the effect of such an examination is when in real time the conclusion may be drawn whether or not the data from the tested object indicate the damage, even in the cases when the damage occurs during the operation of the tested object.

It is of utmost importance that the data supporting the algorithm in the field of stationary signals are analyzed properly. The important parameters are as follows: the order of the ARMA model, the length of the data windows, and the test if the residuals obtained are normal, impeded, and identically distributed. Verification of the construction condition has to be based on the proper baseline (the same environmental conditions). In addition, the proposed solution presents current and modern approaches to solving the problem. In particular, it offers the following:

(i) The effective separation of stationary and non-stationary signals
(ii) Optimal ARMA model parameters
(iii) Implementation possibilities supporting online solutions by limiting computational complexity
(iv) Effective input data for the analyzes conducted using the AI method, in particular for classifying the DSF parameters and Cook's distances assigned to them
(v) A methodology of using Hilbert transforms for oversize excitations
(vi) The use of observation methods based on interferometric radars, which facilitate the location of potential damage, because the input data are uniform in the time domain and strictly defined to the location; due to the easy coverage of the tested object with multiple observations, the analysis of data, and consequently the location of the damage, is easier
(vii) Input data from radar systems which allow, due to the frequency and accuracy of the displacement measurements, the use of the most algorithms that were developed for the analysis of the measurements performed with the accelerometers
(viii) No influence of weather conditions variability on the possibility of inference about the state of the object for the dynamic issues.

Further research is the technological implementation of machine learning which will allow for the automatic classification of the DSF coefficients.

Data Availability

The PDF data used to support the findings of this study are included within the supplementary information file(s).

Conflicts of Interest

The authors declare that there are no conflicts of interest regarding the publication of this paper.

Acknowledgments

This publication was prepared within statutory research fund no. 11.11.150.005 of the Department of Engineering Surveying and Civil Engineering, Faculty of Mining Surveying and Environmental Engineering of AGH University of Science and Technology in Kraków.

Supplementary Materials

Raw radar measurement data have been provided as a supplementary material in the form of a PDF file. (*Supplementary Materials*)

References

[1] V. Gikas, "Ambient vibration monitoring of slender structures by microwave interferometer remote sensing," *Journal of Applied Geodesy*, vol. 6, no. 3-4, pp. 167–176, 2012.
[2] C. Gentile and G. Bernardini, "Output-only modal identification of a reinforced concrete bridge from radar-based measurements," *NDT & E International*, vol. 41, no. 7, pp. 544–553, 2008.
[3] R. C. Barros and F. M. Paiva, "On the use of radar interferometry for the structural monitoring of bridges," in *Proceedings of the 6th International Conference Integrity-Reliability-Failure (IRF2018)*, pp. 1287–1300, Lisbon, Portugal, July 2018.
[4] M. Diaferio, A. Fraddosio, M. D. Piccioni, A. Castellano, L. Mangialardi, and L. Soria, "Some issues in the structural health monitoring of a railway viaduct by ground based radar interferometry," in *Proceedings of the IEEE Workshop on Environmental, Energy, and Structural Monitoring Systems (EESMS)*, pp. 1–6, IEEE, Milan, Italy, July 2017.
[5] P. Kohut, K. Holak, T. Uhl et al., "Monitoring of a civil structure's state based on noncontact measurements," *Structural Health Monitoring: An International Journal*, vol. 12, no. 5-6, pp. 411–429, 2013.
[6] J. Hu, J. Guo, L. Zhou, S. Zhang, M. Chen, and C. Hang, "Dynamic vibration characteristics monitoring of high-rise buildings by interferometric real-aperture radar technique: laboratory and full-scale tests," *IEEE Sensors Journal*, vol. 18, no. 15, pp. 6423–6431, 2018.
[7] A. Castellano, A. Fraddosio, F. Martorano, G. Mininno, F. Paparella, and M. D. Piccioni, "Structural health monitoring of a historic masonry bell tower by radar interferometric measurements," in *Proceedings of the IEEE Workshop on Environmental, Energy, and Structural Monitoring Systems (EESMS)*, pp. 1–6, IEEE, Salerno, Italy, June 2018.
[8] F. X. Ochieng, C. M. Hancock, G. W. Roberts, and J. Le Kernec, "A review of ground-based radar as a noncontact sensor for structural health monitoring of in-field wind turbines blades," *Wind Energy*, vol. 21, no. 12, pp. 1435–1449, 2018.
[9] C. R. Farrar and K. Worden, *Structural Health Monitoring. A Machine Learning Perspective*, John Wiley & Sons, Chichester, UK, 2013.
[10] H. Wenzel, *Health Monitoring of Bridges*, John Wiley & Sons, Chichester, UK, 2009.
[11] A. Vetrivel, M. Gerke, N. Kerle, F. Nex, and G. Vosselman, "Disaster damage detection through synergistic use of deep learning and 3D point cloud features derived from very high resolution oblique aerial images, and multiple-kernel-learning," *ISPRS Journal of Photogrammetry and Remote Sensing*, vol. 140, pp. 45–59, 2018.
[12] D. Feng and M. Q. Feng, "Computer vision for SHM of civil infrastructure: from dynamic response measurement to damage detection—a review," *Engineering Structures*, vol. 156, pp. 105–117, 2018.
[13] L. Long, S. Thöns, and M. Döhler, "The effects of SHM system parameters on the value of damage detection information," in

Proceedings of the 9th European Workshop on Structural Health Monitoring (EWSHM), pp. 1–10, Manchester, UK, July 2018.

[14] Y.-L. Zhou, N. M. Maia, and M. Abdel Wahab, "Damage detection using transmissibility compressed by principal component analysis enhanced with distance measure," *Journal of Vibration and Control*, vol. 24, no. 10, pp. 2001–2019, 2018.

[15] B. Zhang, Y. Qian, Y. Wu, and Y. B. Yang, "An effective means for damage detection of bridges using the contact-point response of a moving test vehicle," *Journal of Sound and Vibration*, vol. 419, pp. 158–172, 2018.

[16] J. Huang, D. Li, H. Li, G. Song, and Y. Liang, "Damage identification of a large cable-stayed bridge with novel cointegrated Kalman filter method under changing environments," *Structural Control Health Monitoring*, vol. 25, no. 5, article e2152, 2018.

[17] B. Bhowmik, M. Krishnan, B. Hazra, and V. Pakrashi, "Real-time unified single- and multi-channel structural damage detection using recursive singular spectrum analysis," *Structural Health Monitoring*, vol. 18, no. 2, pp. 536–589, 2018.

[18] T. B. Roy, S. Banerji, S. K. Panigrahi, A. Chourasia, L. Tirca, and A. Bagchi, "A novel method for vibration-based damage detection in structures using marginal Hilbert spectrum," in *Recent Advances in Structural Engineering, Vol 1*, A. Rao and K. Ramanjaneyulu, Eds., vol. 11, pp. 1161–1172, Lecture Notes in Civil Engineering, Springer, Berlin, Germany, 2019.

[19] M. Krishnan, B. Bhowmik, B. Hazra, and V. Pakrashi, "Real time damage detection using recursive principal components and time varying auto-regressive modeling," *Mechanical Systems and Signal Processing*, vol. 101, pp. 549–574, 2018.

[20] H. Sohn, C. Farrar, H. Hunter, and K. Worden, "Applying the LANL statistical pattern recognition paradigm for structural health monitoring to data from a surface-effect fast patrol boat," Technical Report LA-13761-MS, Los Alamos National Laboratory, Los Alamos, NM, USA, 2001.

[21] K. K. Nair, A. S. Kiremidjian, and K. H. Law, "Time series-based damage detection and localization algorithm with application to the ASCE benchmark structure," *Journal of Sound and Vibration*, vol. 291, no. 1-2, pp. 349–368, 2006.

[22] K. Shin and J. K. Hammond, *Fundamentals of Signal Processing for Sound and Vibration Engineers*, John Wiley & Sons, Chichester, England, 2008.

[23] G. E. P. Box and D. A. Pierce, "Distribution of residual autocorrelations in autoregressive-integrated moving average time series models," *Journal of the American Statistical Association*, vol. 65, no. 332, pp. 1509–1526, 1970.

[24] T. Owerko, "Method of prototyping sensitive dynamic engineering structures supporting automatic information identification regarding a structure's condition," *Journal of Civil Engineering and Architecture*, vol. 10, no. 8, pp. 912–918, 2016.

[25] Ž. Nakutis and P. Kaškonas, "Bridge vibration logarithmic decrement estimation at the presence of amplitude beat," *Measurement*, vol. 44, no. 2, pp. 487–492, 2011.

[26] T. Owerko, "Beat frequency detection of bridges using ground-based radar interferometry," *Measurement Automation Monitoring*, vol. 60, no. 11, pp. 1065–1068, 2014.

[27] R. D. Cook, "Influential observations in linear regression," *Journal of the American Statistical Association*, vol. 74, no. 365, pp. 169–174, 1979.

[28] M. Pieraccini, M. Fratini, F. Parrini, G. Macaluso, and C. Atzeni, "High-speed CW step-frequency coherent radar for dynamic monitoring of civil engineering structures," *Electronics Letters*, vol. 40, no. 14, pp. 907-908, 2004.

[29] S. Rödelsperger, "Real-time processing of ground based synthetic aperture radar (GBSAR) measurements," in *Schriftenreihe Fachrichtung Geodäsie*, no. 33, Fachbereich Bauingenieurwesen und Geodäsie, Technische Universität Darmstadt, Darmstadt, Germany, 2011.